JOURNAL OF PROPULSION AND POWER
Vol. 13, No. 1, January–February 1997

Analytical Model of Unsteady Shock Motion on Hypersonic Forebodies

Sowmyalatha Jayaraman* and Mark J. Lewis†
University of Maryland, College Park, Maryland 20742

The behavior of an unsteady shock associated with the surface of the forebody of a hypersonic vehicle is modeled analytically. The present study develops a simple engineering model, based on the nonlinear oscillator theory, to perform a dynamic analysis on nonuniform flow over two-dimensional hypersonic forebodies. The emphasis is on exploring the fluid physics while avoiding time-intensive computational techniques for unsteady calculations. Closed-form solutions of the shock motion are derived and any coupling phenomena between the boundary layer and the shock are studied by including viscous effects in the analysis. The response of the shock to different freestream Mach numbers, frequencies, and amplitudes of perturbation is examined. A quasisteady approach and piston analogy have been incorporated. It is shown that the amplification factor of the inviscid shock relative to the surface matches with the computational results within 10% accuracy under similar conditions.

Nomenclature

A = amplification factor
a = speed of sound, m/s
F = perturbation force, N
f = perturbation frequency, 1/s
K = stiffness of the oscillator, N/m
K_{eq} = equivalent spring constant, N/m
L = wedge length, m
M = Mach number
$\mathcal{M}$ = mass of the oscillator, kg
P = pressure, N/m^2
Q = forcing function
t = time, s
U = flow velocity, m/s
y = displacement from the mean position, m
β = shock-wave angle
γ = ratio of specific heats
δ = boundary-layer displacement thickness, m
θ = wedge angle, rad
ν = Strouhal number
ρ = density, kg/m^3
ϕ = included angle of the oscillator, rad
ω = circular frequency, 1/rad

Subscripts
b = boundary layer
i = inviscid layer
w = wedge
0 = initial conditions
∞ = freestream

Introduction

DESIGN of the forebody of a hypersonic vehicle has a major impact on the inlet compression process and, hence, the overall performance of the vehicle. An important design criterion is the matching of the inlet bow shock with the cowl lip. For a steady analysis of the vehicle in Fig. 1, the matching criteria can be accurately satisfied.[1] However, for a hypersonic vehicle subjected to various external perturbations, the effect of the unsteady phenomena on the inlet flowfield and control of the shock motion become important considerations.

If the shock motion were to be identical to the surface motion, then the bow shock would move in phase with the surface. Any difference in the amplitude or phase of the motion would result in a displacement of the shock from the engine cowl. It becomes pertinent to determine the existence of certain conditions that lead to substantial departures from the ideal behavior and, if such conditions do exist, then their effect on the overall performance of the forebody has to be analyzed. For the type of slender forebody shapes currently envisioned for hypersonic vehicles, even a small divergence of the shock angle could result in large relative deflections downstream close to the engine cowl.

There has been a large body of research in oscillatory wedge flows in conjunction with flutter, buzzing, and mixing augmentation for scramjet propulsion using the piston theory or solving for the linearized small perturbation equations or the Euler or full Navier–Stokes equations. By analyzing the unsteady supersonic flow over a wedge, Carrier[2] found that the weak shock solution is not appreciably altered by the shock boundary condition omission and determined the criteria for detachment of the shock from the leading edge for high frequencies of oscillation. This theory was carried over by Van Dyke[3] to study the effect of pivotal points of oscillation other than the leading edge, i.e., for plunging motion of the wedge.

Lighthill[4] proposed a physical model that simplified the analysis of high-speed unsteady aeroelastic problems. Adopting Hayes',[5] argument, Lighthill[4] propounded a simple theory that at high Mach numbers could yield accurate results for the pressure distribution on a surface, even for large-amplitude perturbations. Landahl[6] developed this model utilizing higher expansion powers for the thickness of the surface and the inverse of Mach number. Ashley and Zartarian[7] developed the piston theory to obtain closed-form solutions for the bending-torsion and control-surface flutter properties of airfoils at high Mach numbers. It is pointed out that a Mach number zone exists with appreciable thermal effects, but negligible nonlinear viscous interactions, wherein accurate estimates of aerodynamic–thermoelastic problems can be obtained. Morgan et al.[8] gave a vivid comparison of the various theories available

Presented as Paper 95-2771 at the AIAA/ASME/SAE/ASEE 31st Joint Propulsion Conference and Exhibit, San Diego, CA, July 10–12, 1995; received Sept. 22, 1995; revision received June 1, 1996; accepted for publication June 6, 1996.

*Graduate Research Assistant, Department of Aerospace Engineering. Student Member AIAA.

†Associate Professor, Department of Aerospace Engineering. Associate Fellow AIAA.

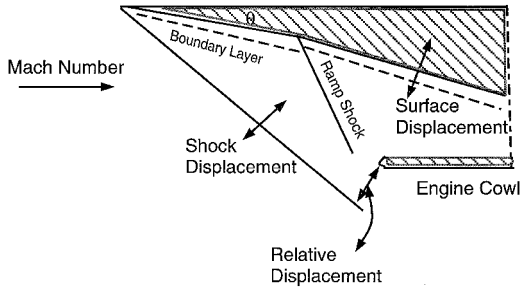

Fig. 1 Generic hypersonic forebody.

for predicting the aeroelastic effects and concluded that the piston theory compared very well with the exact theories.

An exact unified theory for both hypersonic and supersonic flows past an oscillating wedge of arbitrary thickness, with the assumptions of attached bow shock and small perturbations by solving the exact linearized perturbation equations for low- and high-frequency regimes, was developed by Hui.[9,10] The results included the stability criterion put forward by McIntosh.[11] Hui[9,10] also derived exact closed-form solutions for the stability derivatives of the pitching caret wings at design conditions for hypersonic flow. A similar approach was later adopted by Chavez and Liu[12] to develop a perturbed Euler characteristics method for the entire frequency domain.

A computational solution of the unsteady wedge problem by Lewis et al.[13] shows that the overall shock motion is nonlinear. A wedge of 30 m and freestream Mach numbers from 5 to 20 were considered. The shock was unaffected by the wedge motion at high frequencies ($\geq$1000 Hz), while the shock amplitude was the driving amplitude at low frequencies ($\approx$20 Hz). At intermediate frequencies ($\approx$100 Hz), a resonance of sorts was reached, with the amplitude substantially greater than the driving motion. This behavior has been suggested to resemble the motion of a simple harmonic oscillator, with a nonlinear driving mechanism and a driven system whose mass varies along the wedge.

The present work[14] derives its basis from the results of Lewis et al.[13] The focus is on replacing time-intensive computational techniques with simple analytical theories with a minimum loss of precision.

Formulation of the Model

The wedge flow is modeled as a nonlinear oscillator with a variable mass. The generic hypersonic forebody/inlet is idealized to be a slender wedge of fixed inclination to the freestream. The entire flowfield is assumed to be two dimensional and devoid of any chemical reactions. The shock is always attached to the leading edge, neglecting the low-density effects on the flow.

Consider a wedge of length L, at an angle of attack α to the freestream in the steady state, with a bow shock attached to the leading edge as shown in Fig. 2. Any unsteady perturbation normal to the surface will be transmitted to the shock, and thus induce a motion that may be in- or out-of-phase with the surface motion. The transient flowfield properties in the flow direction are assumed to be almost equal to that of the steady-state values or those at low frequencies of oscillation. This is because the flow velocity is very large compared to the perturbation velocity, normal to the surface. Therefore, any slight variations in the transient properties of the flow, in the flow direction, can be safely ignored. The analytical model is thus a two-dimensional model with the flow analysis confined to the plane normal to the flow. It is then justifiable to interpret the flow encompassed between the wedge surface and the shock as an oscillator whose mass and size increase as a function of time. The size is qualified either by a reference height or area of the oscillator. The flow time is defined by the geometry of the wedge and is given by $t_0 = L/U_0$, where U_0 is

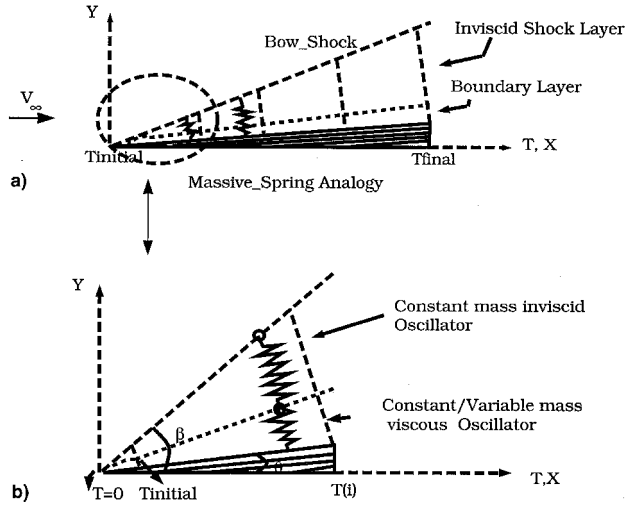

Fig. 2 Oscillator model.

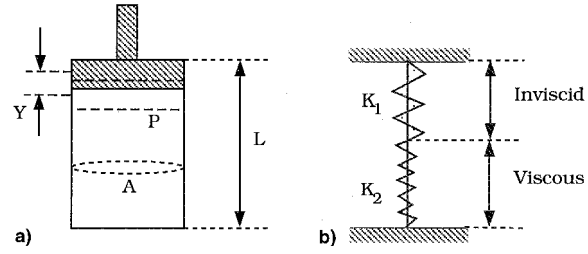

Fig. 3 Oscillator analogy: a) spring of air and b) oscillator model.

the flow velocity along the wedge. The unsteady effects are introduced into the problem through a driving function.

Massive Spring Analogy

Figure 2a depicts the oscillator at a time $t(i)$ along the wedge. An analogy is drawn between an infinitesimally thin column of fluid and a massive uniform spring of total mass $\mathcal{M}$ and spring constant K. The spring constant defines the stiffness or the quality of springiness in the fluid column. Figure 2b shows the event enlarged at time $t(i)$ for a viscous model; the oscillator system comprises two springs of spring constants K_1 and K_2 representing the inviscid and viscous layers, respectively.

The variation between the massless spring and its massive counterpart is reflected in their natural frequency of oscillations; the massive oscillator is nothing but a massless spring with a third of its total mass M added to its end. Since there is no distribution of mass along the fluid column,[15] normal to the flow direction, every point along the fluid column experiences the same stretching force. Therefore, the oscillator becomes the repository of all the kinetic and elastic potential energy. For this simplified case, the natural frequency of vibration of the massive oscillator is

$$\omega_n^2 = \frac{K}{M/3} \tag{1}$$

Spring Constant

The spring constant of the oscillator can be related to the quality of stiffness or compressibility of the flow and defined in terms of the force acting on the system per unit length. The wedge-driven motion of the fluid is similar to that of a piston driving a column of fluid in a tube (Fig. 3a) closed at one end. The entrapped column of fluid acts like a strong spring, very resistant to sudden pull or push. For this system, it can be shown that, under adiabatic conditions, the spring constant is a function of the cross-sectional area, pressure, and the time-

dependent length of an equivalent fluid column and the angle subtended by the oscillator.

Force Equilibrium

At any instant, the factors contributing to the force on the oscillator system are its mass and stiffness and the external perturbation force acting on it. The balanced force equation can then be given by

$$\mathcal{M}(t)\frac{d^2y}{dt^2} + 3K(t)y = F(t) \tag{2}$$

where y is the displacement of the oscillator from its steady-state equilibrium position, $M(t)$ is the time-dependent mass of the system, $K(t)$ is the time-varying spring constant, and the quantity $F(t)$ represents the perturbation force as a function of time. Since the entire mass of the oscillator is concentrated at its end, y also denotes the displacement of the shock from its steady-state equilibrium position. Equation (2) is a linear equidimensional ordinary differential equation if mass varies linearly.

Mass-Flux Model

A simplistic model describing the mass flux as a function of time, purely based on geometry, is a linear model:

$$\mathcal{M}(t) = \mathcal{M}_0(t/t_0) \tag{3}$$

However, any unsteady perturbation of the system results in an inflow or outflow of mass into the shock layer because of the displacement of the shock. To account for this additional mass flow and any shock curvature caused from the leading-edge bluntness, power-law profile for mass flux is used. In this case, the mass of the system is given by

$$\mathcal{M}(t) = \mathcal{M}_0(t/t_0)^n \tag{4}$$

Analytical Solutions

Three cases of the driving function are considered, that of a time-independent function $F(t) = F_0$, and linearly and periodically time-varying functions $F(t) = F_0t$ and $F(t) = F_0 \sin \omega t$.

To characterize the flowfield, the variables in Eq. (2) can be combined to form nondimensional constants. Therefore, nondimensionalizing y, t, and the frequency of perturbation f, with respect to a reference length L, the length of the wedge, a reference time t_0, the flow time, and a reference frequency f_0, which is equal to $1/t_0$, the model equation takes the form

$$t^2\frac{d^2y}{dt^2} + C_{1y} = C_2tF \tag{5}$$

The Strouhal number ν characterizes the nature of the oscillating flows. It is physically the ratio of the residence time to oscillation time. When it is small, the flow has time to adjust to the changes brought about by the oscillations, which is the low-frequency domain. A higher value of Strouhal number corresponds to the high-frequency domain, wherein the flow time is much greater than the oscillation time. It is defined as $\nu = f_0L/U_0$. C_1 and C_2 are two constants independent of time and defined as,

$$C_1 = \frac{6\gamma P}{\rho u^2 \tan^2\phi}, \qquad C_2 = \frac{2P}{\rho u^2 \tan\phi} \tag{6}$$

where $\phi = \beta - \theta$.

The values of C_1 and C_2 for different freestream Mach numbers are shown in Fig. 4. The oscillator model can be essentially characterized by the two constants C_1 and C_2. While C_1 models the inertia of the oscillator mass and its compressibility,

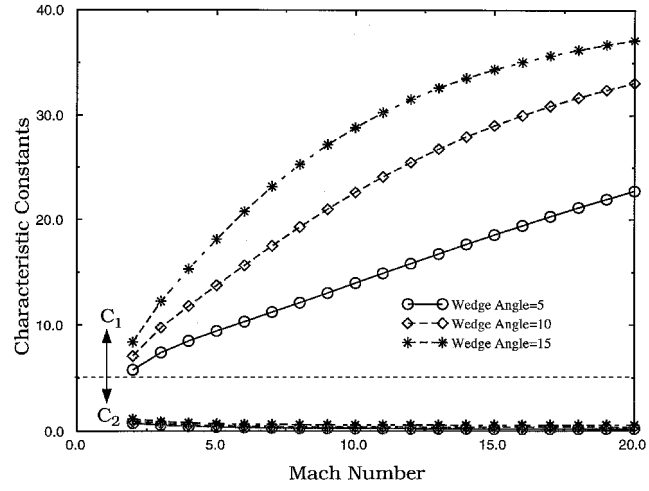

Fig. 4 Variation of C_1 and C_2 with Mach number.

C_2 emulates the perturbation and the effect of unsteadiness because of it.

Closed-form solutions are obtained for particular cases of constant and linear force inputs. For the linear mass flux model, depending on the value of C_1, which describes the natural frequency of the mass-spring system,[14] the solution takes the form

$$y = t^{1/2}(AC + BD) + Q(t) \tag{7}$$

The particular solution involves the force function and takes the form 1) $Q(t) = D_1t$ for a constant input force, 2) $Q(t) = D_2t^2$ for a linear input force, and 3) $Q(t) = D_3t \sin \omega t + D_4t \cos \omega t$ for a sinusoidal force; where A, B, C, D, D_1, D_2, D_3, and D_4 are functions of time and are given by

$$D_1 = F_0(C_2/C_1) \tag{8}$$

$$D_2 = F_0[C_2/(C_1 + 2)] \tag{9}$$

$$D_3 = \frac{F_0C_2(C_1 - \omega^2t^2)}{(C_1 - \omega^2t^2)^2 + 4\omega^2t^2} \tag{10}$$

$$D_4 = \frac{-2\omega t}{C_1 - \omega^2} \tag{11}$$

$$C = \cos\{[\sqrt{(4C_1 - 1)}/2]\log(t)\} \tag{12}$$

$$D = \sin\{[\sqrt{(4C_1 - 1)}/2]\log(t)\} \tag{13}$$

and with $p = \sqrt{(4C_1 - 1)}/2$

$$A = M(S + pC) - NS/p \tag{14}$$

$$B = NC - M(C - pS)/p \tag{15}$$

Where, for constant perturbation force

$$M = \sqrt{t}[\tan\phi - F_0(C_2/C_1)] \tag{16}$$

$$N = -2\sqrt{t}F_0(C_2/C_1) \tag{17}$$

For linear time-varying force

$$M = \sqrt{t}\{\tan\phi - F_0[C_2/(C_1 + 2)t]\} \tag{18}$$

$$N = -4F_0[C_2/(C_1 + 2)]t\sqrt{t} \tag{19}$$

The case of sinusoidal force input involves higher powers of t and its derivatives. It is solved using a fourth-/fifth-order

Runge–Kutta solver. The wedge displacement is obtained by incorporating either the piston or quasisteady approach.

Viscous Effects

The effects of viscosity become prominent with the inclusion of the boundary layer in the analysis. Three cases have been considered building upon the mass flux and spring constant models.

Mass Flux Model

At high Mach numbers for laminar boundary layers, there is very little mass flux in the boundary layers.[16] This is because the streamlines entering the boundary layer cross the leading-edge shock wave at points far upstream and much closer to the leading edge. The viscous effects are, thus, predominant only in a very small region. However, in reality, there is a mass flow variation across the boundary layer because of varying velocity and temperature and, hence, density caused by the no-slip condition. Therefore, two cases of the mass model have been attempted.

1) Model 1: the mass flow entrained in the boundary layer is a constant.[16]

2) Model 2: the density profile in the boundary layer corresponds to a power law.

The two oscillators in each model are subjected to uniform external force. The mass flow variation in the viscous model 2 is treated in layers or strata across the boundary layer. The power law for density profile is

$$\rho/\rho_0 = (y/\delta)^n \tag{20}$$

where n is the power index.

Assuming constant mass flow in the boundary layer, for model 1, Eq. (5) becomes

$$\frac{d^2y_b}{dt'^2} + C\frac{y_b}{\sum_0^\delta (y_b/\delta)^n} = D\frac{F}{\sum_0^\delta (y_b/\delta)^n} \tag{21}$$

with

$$C = 6\gamma P/\rho u^2\delta^2, \qquad D = 2FP/\rho u^2\delta \tag{22}$$

where y_b is the nondimensional displacement of the boundary layer from its equilibrium position. Denoting $s = L\tan\phi - \delta$, the displacement of the inviscid shock layer, with a linear mass flow profile, is described by

$$\frac{d^2y_i}{dt^2} + C\frac{y_i}{t^2} = \frac{DF}{t} \tag{23}$$

with $C = 2\gamma PL^2/\rho u^2 s^2$ and $D = 2FPL/\rho u^2 s$.

Equivalent Spring Constant

Viscous model 3 assumes two massive springs in series (Fig. 2b), one for the boundary layer and the other for the inviscid shock layer between the boundary layer and the shock. The spring constant for this model is obtained by applying the resistor analogy. If K_1 and K_2 represent the spring constants of the inviscid and viscous oscillator, then the equivalent spring constant is

$$K_{eq} = K_1K_2/(K_1 + K_2) \tag{24}$$

Results and Discussion

The wedge model considered is 30 m long and the included angle is 5 deg.[13] The freestream conditions are shown in Table 1. The frequency of the forcing function ranges from a low frequency of 5 Hz to a high-frequency value of 100 Hz. (Unless specified otherwise, all results are shown plotted in the nondimensional domain.)

Table 1 Freestream conditions

Freestream parameter	Value
Static pressure	21 N/m^2
Static temperature	254.6 K
Density at 60 km	0.0002874 kg/m^3

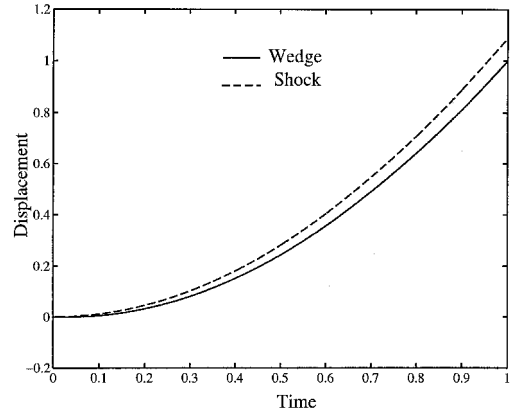

Fig. 5 Absolute motion of the oscillator: $M = 10$, $f = 10$ Hz, and $A = 0.1$.

Amplitude of the Driving Function

For a steady-state analysis with a freestream Mach number of 5, the included angle between the bow-shock and the wedge ϕ is approximately 0.175 rad. For a quasisteady behavior, any displacement of the oscillator caused by the oscillation function does not deviate significantly from the steady-state value. Therefore, any variation in the angle is a direct result of the unsteadiness introduced into the system by the perturbation force. It is observed that there is a very small deviation of the oscillator angle from its steady-state value for amplitudes ranging from 0.001 to 1, which gives a measure of the amplitude of the input forcing function.

Inviscid Model

An additional tuning parameter with a sinusoidal driving function is the Strouhal number, which gives a measure of the residence time of the fluid to the time for oscillation. The low-frequency domain would then correspond to the case of a small Strouhal number, i.e., when the flow has time to adjust to any variation induced by the unsteadiness. For the given wedge configuration, the flow time, which is the time taken by the fluid to make one sweep over the wedge, is approximately 0.02 s for a freestream Mach number of 5. This is the time span during which the effect of unsteadiness on the wedge flow is considered. Extending this further, note that for the flow to perceive at least one cycle of oscillation, the frequency of oscillations should be of the order of or greater than 50 Hz. When a linear mass flux is incorporated into the oscillator model and the amplitude of perturbation force is 0.1, Eq. (2) for the inviscid model can be rewritten as Eq. (5).

Shock-Wedge Response

The shock and the wedge motion for a freestream Mach number of 10 and a perturbation frequency of 10 Hz are shown in Fig. 5. The ordinate refers to the relative motion between the wedge and the shock. The amplification factor of the shock and the wedge motion for this case is $A = 0.88$. Similarly, the amplification factor for a lower Mach number of 5 and perturbation frequency 5 Hz is found to be $A = 0.7854$. The Strouhal number for both cases is less than unity. These results

match those reported by Lewis et al.[13] They also show an in-phase motion between the shock and the wedge with an amplification factor of 0.8 for a Mach 10 and frequency 10-Hz flow condition, thus predicting a quasisteady behavior. The discrepancy in the present and the computational values could be attributed to an initial mass flux loss caused by the limitation of the model at zero time. The lower mass flux thus imparts a lower frequency of oscillation, thereby reducing the relative magnitudes of the shock and the wedge. For the lower Mach number of 5, the amplification factor is less than unity, resulting in a small overall increase in the amplitude of the relative motion.

Frequency vs Time

All of the results obtained earlier display a time variation of frequency, i.e., the frequency of oscillations is seen decreasing with increasing time. Figure 6 shows the time-frequency plot for a Mach 10 and a perturbation frequency of 10 flow conditions. The behavior of the oscillator is one of divergence with an increasing amplitude and decreasing dominant frequencies. From an energy perspective, this can be attributed to the redistribution of the overall energy between the kinetic and the potential energy of the fluid particles. The reduction in the frequency of oscillations of the massive system results from decreasing kinetic energy of the unsteady flow. Similar behavior is exhibited over a wide range of frequencies.

Frequency Spectrum

The frequency of the shock motion is analyzed in Fig. 7, which is a plot of the spectral density as a function of the Strouhal number for a Mach 5 and frequency 5-Hz case. The shock response at approximately 0.2 s is considered. (Figure 7 shows the zoomed-in region where the peak occurs.) The Nyquist frequency for this case is 50 Hz. It is found that the peak frequency of the shock is around 0.1, which is approximately equal to the Strouhal number of the forcing oscillations ($\nu = 0.09847$). The amplitude of the perturbation force is taken to be 0.1. Varying the amplitude of the force only changes the magnitude of the resultant displacement of the oscillator and produces little or no change in the phase relation as referred to in the previous sections. Similar results are obtained for the case of the Mach 10 and frequency 10-Hz flows, the only difference being a smaller displacement of the shock.

Surface Pressure Distribution

The unsteady surface pressure distribution over the wedge is evaluated at each time.[14] For a Mach number of 5 and frequency of 5 Hz, the ratio of the unsteady logarithmic pressure to that of the steady-state value is plotted at three instances against the logarithm of the distance along the wedge in Fig. 8. The surface pressure decreases with increasing time. As the Mach number of the flow is increased, the unsteady surface pressure, at any axial location, is seen fluctuating about its steady-state value. A similar behavior is exhibited for increasing frequencies of perturbation.

Using the tangent wedge theory, the coefficient of pressure along the surface can be plotted. Figure 9 shows the *Cp* distribution along the wedge for a range of Mach numbers. The previous results are compared with those obtained by Chavez and Liu.[12] At high Mach numbers, with a smaller aft-shock Mach wave angle, they report weak interaction between the Mach waves and shock, and the pressure distribution is devoid of any waviness. Figure 9 exhibits a similar behavior.

Viscous Model

The addition of viscosity does not affect the overall bulk behavior of the flowfield at low frequencies. The most striking feature of the viscous model is the displacement effect caused by the presence of the boundary layer. For a Mach number of

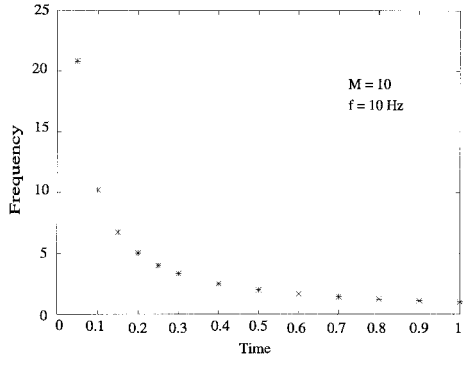

Fig. 6 Inviscid model: frequency vs time.

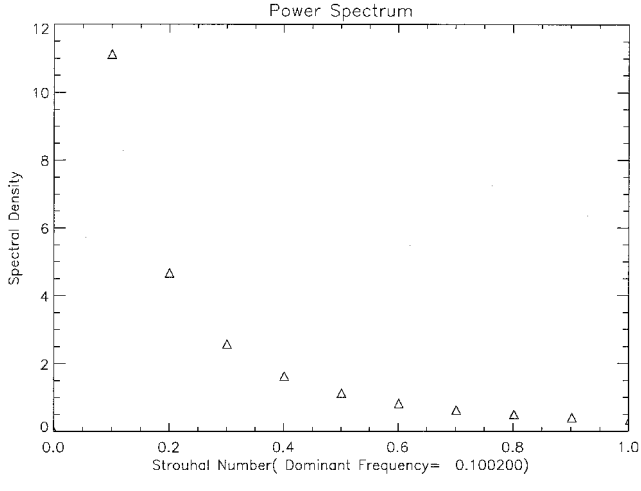

Fig. 7 Frequency spectrum: $M = 5$, $f = 5$ Hz, and $A = 0.1$.

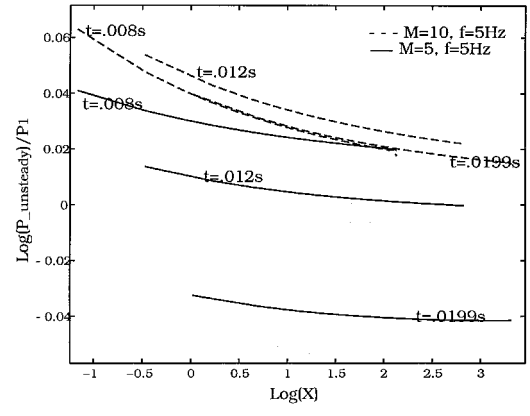

Fig. 8 Surface pressure distribution: $A = 0.1$.

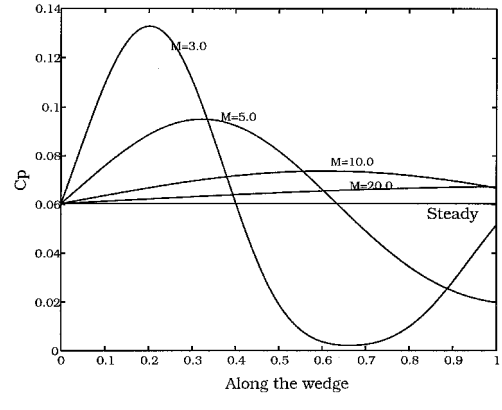

Fig. 9 *Cp* distribution: $f = 50$ Hz and $A = 0.1$.

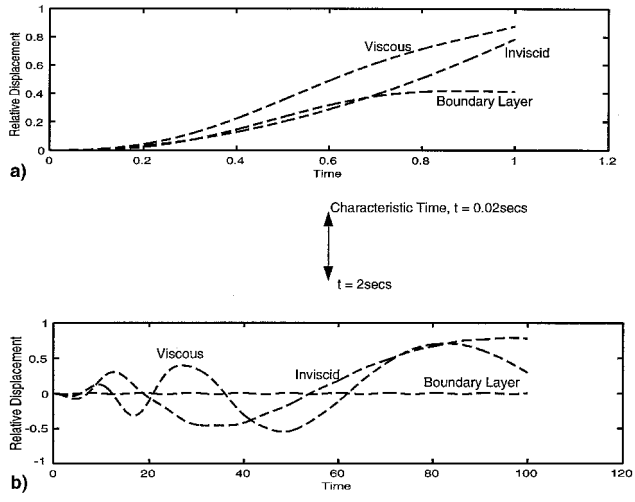

Fig. 10 Viscous model (rigid boundary layer): $M = 5, f = 5$ Hz, $A = 0.1$, and $n = 2$.

5 and frequency of oscillation 5 Hz, the inviscid and viscous shock motion, assuming constant mass flux in the boundary layer, are plotted in Fig. 10. Figures 10a and 10b depict the relative displacement of the viscous and the inviscid shock. Also shown in the figures is the displacement of the boundary layer about its steady-state equilibrium position. Figure 10b gives the qualitative behavior of the shock and the boundary layer for a length 100 times longer than the wedge length, i.e., for a characteristic time $t = 2$ s.

The presence of the boundary layer further displaces the shock from its mean position. The viscous shock is in-phase with the inviscid case and its amplification factor with respect to the wedge surface is,

$$A_{\text{viscous}} = 1.115A_{\text{inviscid}} \tag{25}$$

The amplification factor of the viscous shock is compared with that of the inviscid case over a wide range of frequency in Figs. 11–13 for two values of Mach number and for the three viscous models. From the formulation of the viscous models, a wide disparity in behavior is noted between the rigid and stratified boundary-layer models. For the same amplitude of perturbation, the following are observed.

1) The ratio of the amplitudes of the viscous and the inviscid shock, for the rigid model, is substantially lower compared to the stratified assumption.

2) There are certain frequencies at which the amplification factor of the viscous to the inviscid shock, for a rigid model, has the same value for different freestream Mach numbers.

3) The stratified boundary layer deflects the viscous shock by almost a constant factor, though large, when the Mach number is increased at low frequencies. This value, however, decreases as the frequency of perturbation was increased.

4) Ignoring any density variations in the viscous model, i.e., when the effects of stiffness alone are considered, the model shows similar behavior as the rigid model at low frequencies and as the stratified model at higher frequencies.

Displacement Model

A variation to the previous model is formulated by employing displacement as the driving function. An equivalent force on the wedge is determined using the piston theory and is included in the oscillator model. The perturbation force acting on the oscillator is given by

$$F(t) = \int_{t_{\text{init}}}^{t} [1 \pm h\cos(2\pi\nu t)]\,\mathrm{d}t \tag{26}$$

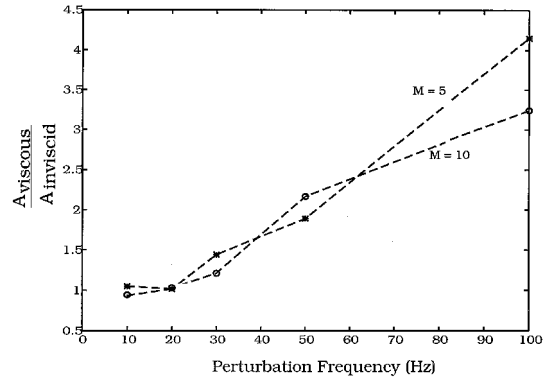

Fig. 11 Viscous model 1.

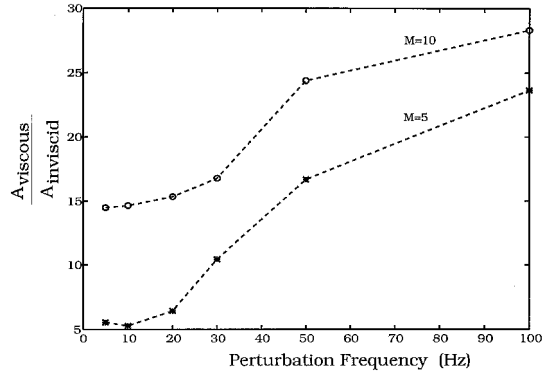

Fig. 12 Viscous model 2.

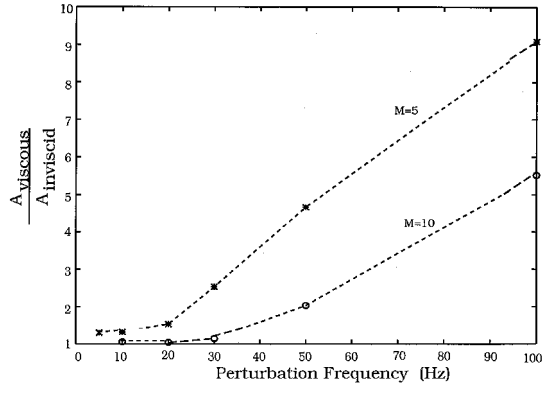

Fig. 13 Viscous model 3.

where $h = 2\pi\nu A\gamma/at_0$, with A denoting the amplitude of displacement. When the shock moves towards the surface, an isentropic compression occurs and vice versa if the shock moves away from the surface. This is interpreted in the present model as

$$\text{if} \quad \frac{\mathrm{d}y_w}{\mathrm{d}t} > 0 \rightarrow \text{isentropic compression}$$

$$\text{if} \quad \frac{\mathrm{d}y_w}{\mathrm{d}t} < 0 \rightarrow \text{isentropic expansion}$$

Figure 14 shows the amplification factor for a wide frequency spectrum. It is observed that the amplification factor decreases as frequency increases. For the higher frequencies of perturbation, the expansion and compression waves generated by the surface occur at a higher rate, thus cancelling at a lower characteristic length above the surface. As a result, the disturbance is cancelled before it affects the shock. In such a

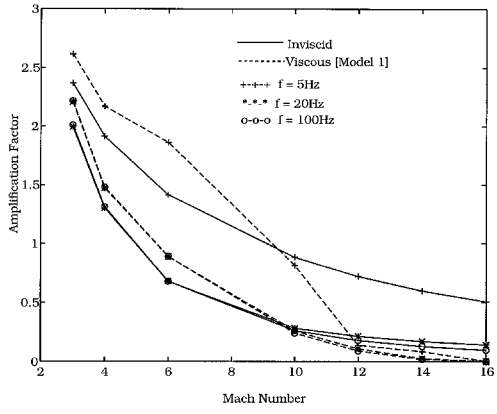

Fig. 14 Displacement model: amplification factor vs Mach number.

situation, the shock shows little or no displacement about its steady-state equilibrium position. This behavior is exhibited by all three viscous models using piston theory, whereas the quasisteady assumption cannot be applied in these regimes of frequency.

Conclusions

An analytical model of the idealized hypersonic forebody exhibiting plunging/pitching oscillations is formulated using the basic physics of the flow. The resulting behavior of the flowfield is examined. In reality, the source of these disturbances can be attributed to propulsion system operation, structural vibrations, and acoustic loads. The behavior of the model also reflects upon the operation of the forebody as a suitable inlet to an integrated scramjet propulsion system.

The present analysis yields a nearly in-phase motion of the unsteady shock and the surface in the lower frequency spectrum. The effects of viscosity have been studied by considering three different boundary-layer models. The constant mass boundary layer resulted in lesser displacements of the shock from the steady-state mean position compared to the stratified model where density variations were incorporated. The equivalent oscillator system exhibited similar behavior to the constant mass boundary-layer model at lower perturbation frequencies and the stratified boundary-layer assumption at higher frequencies.

This methodology could be extended to wedges of arbitrary geometry and freestream conditions, including three-dimensional effects and wall pressure variations. At moderate frequencies and amplitudes of the forcing function, the generation of finite compression and expansion waves in the direction of the oscillator/shock motion could be modeled and included in the analysis.

Acknowledgments

This work has been supported under NASA Grant NAGw 3715, with Isaiah Blankson as the Technical Monitor, to whom appreciation is expressed.

References

[1]Lewis, M. J., "Designing Hypersonic Inlets for Bow Shock Location Control," *Journal of Propulsion and Power*, Vol. 9, No. 2, 1993, pp. 313–321.

[2]Carrier, G. F., "The Oscillating Wedge in a Supersonic Stream," *Journal of the Aeronautical Sciences*, Vol. 20, No. 16, 1948, pp. 150–152.

[3]Dyke, M. D. V., "On Supersonic Flow Past an Oscillating Wedge," *Quarterly of Applied Mathematics*, Vol. 11, No. 3, 1949, pp. 360–363.

[4]Lighthill, M. J., "Oscillating Airfoils at High Mach Number," *Journal of the Aeronautical Sciences*, Vol. 20, No. 6, 1953, pp. 402–406.

[5]Hayes, W. D., "On Hypersonic Similitude," *Quarterly of Applied Mathematics*, Vol. 5, No. 1, 1947, pp. 105, 106.

[6]Landahl, M. T., "Unsteady Flow Around Thin Wings at High Mach Numbers," *Journal of the Aeronautical Sciences*, Vol. 24, No. 1, 1957, pp. 33–38.

[7]Ashley, H., and Zartarian, G., "Piston Theory—A New Aerodynamic Tool for the Aeroelastician," *Journal of the Aeronautical Sciences*, Vol. 23, No. 12, 1956, pp. 1109–1118.

[8]Morgan, H., Runyan, H., and Huckel, V., "Theoretical Considerations of Flutter at High Mach Numbers," *Journal of the Aerospace Sciences*, Vol. 25, No. 6, 1958, pp. 371–381.

[9]Hui, W. H., "Stability of Oscillating Wedges and Caret Wings in Hypersonic and Supersonic Flows," *AIAA Journal*, Vol. 7, No. 8, 1969, pp. 1524–1530.

[10]Hui, W. H., "Interaction of a Strong Shock with Mach Waves in Unsteady Flow," *AIAA Journal*, Vol. 7, No. 8, 1969, pp. 1605–1607.

[11]McIntosh, S. C., "Hypersonic Flow over an Oscillating Wedge," *AIAA Journal*, Vol. 3, No. 3, 1965, pp. 433–440.

[12]Chavez, F. R., and Liu, D. D., "Unsteady Unified Hypersonic/Supersonic Method for Aeroelastic Applications Including Wave/Shock Interaction," AIAA Paper 93-1317, April 1993.

[13]Lewis, M. J., Surline, Y., and Anderson, J. D., Jr., "An Analytical and Computational Study of Unsteady Shock Motion on Hypersonic Forebodies," AIAA Paper 90-0528, Jan. 1990.

[14]Jayaraman, S., "An Analytical Model of the Non-Uniformities and Unsteady Shock Motion on Hypersonic Forebodies," M.S. Thesis, Univ. of Maryland, College Park, MD, 1995.

[15]French, A. P., "Vibrations and Waves," *The MIT Introductory Physics Series*: W. W. Norton and Co., New York, 1971.

[16]Dorrance, W. H., *Viscous Hypersonic Flow*, McGraw–Hill, New York, 1962.